Efficient white-light emission from Zn2GeO4 nanomaterials

P. Hidalgo , J. Dolado , B. Méndez

P. Hidalgo , J. Dolado , B. Méndez , "Efficient white-light emission from Zn2GeO4 nanomaterials," Proc. SPIE 10919, Oxide-based Materials and Devices X, 109192D (1 March 2019); doi: 10.1117/12.2511254

SPIE.

Event: SPIE OPTO, 2019, San Francisco, California, United States

Efficient white-light emission from Zn_2GeO_4 nanomaterials

P. Hidalgo*, J. Dolado, B. Méndez
Dpto. Física de Materiales, Fac, Ciencias Físicas, Univ. Complutense de Madrid, 28040 Madrid, Spain

ABSTRACT

Zn_2GeO_4 is a novel transparent conductive oxide material, with an ultra-wide band gap of 4.5 eV, and rather good electrical conductivity. Zn_2GeO_4 nano- and microwires grown by a thermal technique show two intense emission bands centered in the UV and VIS region, respectively. In this work, we have studied the correlation between luminescence and structural properties in undoped and Mg doped samples. The waveguiding behavior of the microrods has been assessed by the excitation with a 325 nm laser and analysis of the transmitted light along the structure. The intense white luminescence of Zn_2GeO_4 nanomaterials makes them of interest as efficient phosphors for field emission displays.

Keywords: Zinc Germanate, Polarized Raman spectroscopy, Luminescence, Transparent conductive oxides.

1. INTRODUCTION

Transparent conducting oxides (TCO's), which exhibit both high electrical conductivity and high optical transparency in visible light, are necessary for a variety of optoelectronic applications. Their development is critical to many technologies, moreover when these materials are synthetized as low dimensional structures. To date, metal elements such as Zn, In or Sn ('TCO-cations') are essential for TCO formation and form a frontier in the periodic table that separates themselves from other insulating elements, such as Ge or Si. The TCO-cations are post-transition metal cations with electronic configurations of (n−1) d^{10} ns^0 in the oxide (n is the principal quantum number and should be higher or equal to 4 in order to obtain good electrical conductivities). The spherical spread vacant *s* orbitals of these metal cations form highly dispersed conduction bands (CBs) with small effective electron masses, and consequently contributes to high electron mobility. Alternatively, in order to increase the holes mobility in the valence band, hybridization of the *s* states of (n-1) d^{10} ns^2 cations (for example Ge or Sn) with oxygen 2*p* orbitals would be necessary [1]. Not only binary but also ternary oxides have been explored as TCO materials, being Zn_2GeO_4 with a wide-bandgap (4.5 eV) one of the most promising. Some proposed applications are as phosphors in display technology, such as field emission displays, or UV photodetectors [2]. First experimental results of Zn_2GeO_4 have proved that its luminescence is about 40% higher than that of the ZnO phosphors [3]. In addition, Zn_2GeO_4 has high and stable photocatalytic activities [4]–[6]. Moreover, the Zn_2GeO_4 crystalline structure is formed by corner shared ZnO_4 and GeO_4 tetrahedra forming six member rings, with a smaller ring of ZnO_4 tetrahedra and a larger one consisting of boh ZnO_4 and GeO_4 tetrahedra [7]. This configuration made Zn_2GeO_4 a promising material for application in metal-ion batteries as a high-capacity anode material [8].

Native defects usually play a fundamental role in the physical properties in semiconducting oxides, e.g. optical properties, photocatalytic properties or ionic transport, which is very important for batteries. The proposed native defects in Zn_2GeO_4 are oxygen vacancies (V_O) and interstitial zinc (Zn_i), with a donor character, and zinc vacancies (V_{Zn}) and germanium vacancies (V_{Ge}) as acceptors. They are responsible for the luminescence spectra observed in Zn_2GeO_4 that mainly consist of a broad white-bluish emission band peaked at 2.39 eV (520 nm) and a very sharp emission band centered in the near UV region (3.20 eV) (385 nm) [9]. Some studies have demonstrated how it is possible control these native defects. For example, Z. Liu *et al.* [3] observed an improvement of luminescence properties after annealing under different atmospheres. Other option to control the native defects is to introduce impurities. For example, manganese doping increases the green luminescence of the material and reduces the concentration of Zn_i and V_{Zn} [10].

* phidalgo@ucm.es; phone +34 91394 4790

Oxide-based Materials and Devices X, edited by David J. Rogers, David C. Look, Ferechteh H. Teherani, Proc. of SPIE Vol. 10919, 109192D · © 2019 SPIE
CCC code: 0277-786X/19/$18 · doi: 10.1117/12.2511254

Over the past few years, a variety of synthesis routes have been explored for the synthesis of Zn_2GeO_4 nano/microstructures, including conventional solid-state reaction [5], vapor growth techniques [11] and aqueous processes[12]. In this work, undoped and Mg doped Zn_2GeO_4 nano- and microrods have been grown by a catalyst free thermal evaporation method and their luminescence and waveguiding properties have been investigated. Mg^{2+} ions could modify the optical properties by their interaction with the native defects of this semiconductor without introducing a notable lattice distortion if occupies Zn lattice sites. Moreover, because of the small size of Mg^{2+} ions, they could as well locate as interstitial within the rings, and move easily through the channels of this semiconductor contributing to increase the ionic transport properties for batteries applications. It has been reported that interstitial Zn_i defects into the six-membered rings of Zn_2GeO_4, act as an electron trap leading to a long-lasting photoluminescence (LLP)[11]. This behavior would suggest that Mg^{2+} ions could improve the possibilities of the Zn_2GeO_4 nano- and microwires to act as optical resonators.

2. EXPERIMENTAL

Undoped and doped nano- and microrods were grown by a vapor – solid technique using a mixture of ZnO (Sigma Aldrich 99.9 %), Ge (Goodfellow 99.999%) and C (Sigma Aldrich) in 2:1:2 weight ratios homogenized by a ball milling machine during 5 h. For Mg^{2+} doping, MgO (Strem Chemicals 99.999%) was added before the milling in a 10% weight related to the total ZnO:Ge amount. In both cases, the final powders were compacted to form pellets that were thermal annealed during 8 h at 800ºC under an argon flow of 1.5 $lmin^{-1}$. After the thermal treatment, a significant amount of nano- and microstructures were formed on the pellet by an evaporation-deposition process. This synthesis method has already been used to obtain other Ge-based oxides, such as GeO_2 [13] or In_2Ge2O_7 [14] nanostructures. The products were deposited onto silicon wafers for their further characterization. The morphology and chemical composition have been assessed by a scanning electron microscope (SEM) Leica S440 equipped with a Bruker X-ray energy dispersive spectroscopy mode for microanalysis measurements. X-ray diffraction (XRD) measurements for determining the crystal structure were performed with a Philips X'Pert MRD Pro diffractometer. On the other hand, Raman spectroscopy, micro-photoluminescence (μ-PL) and waveguiding investigations were carried out in a Horiba-Jobin-Ybon optical confocal microscope using a 325 nm He-Cd laser, in which polarizers can be inserted in order to make polarization dependent measurements. Cathodoluminescence (CL) was carried out in a Hitachi S-2500 SEM, at temperatures from 80 K to 300K, equipped with a PMA-12 charge coupled device camera.

3. RESULTS AND DISCUSSION

Zinc germanate is composed of GeO_4 and ZnO_4 tetrahedra (Zn is in two different crystallographic positions) bridged by oxygen atoms in a rhombohedral unit cell (a=b=14.23 Å and c=9.53 Å, $\alpha=\beta= 90^o$ and $\gamma=120^o$). This crystalline structure is reflected in the spatial geometry of nanowires grown and in their physical properties. XRD spectra of the structures show only peaks that correspond to the crystal structure of Zn_2GeO_4 (JCPDS card 00-011-0687). The SEM images of samples (nano- and microwires undoped and doped with Mg) show that they have prismatic hexagonal shape with cross sectional dimensions in the range of 1-2 μm, as it is shown in Figure 1. In Mg doped samples, the cross-sectional dimension is slightly higher than in undoped ones reaching values of up to 5 μm. These microwires are, in both cases, longer than 100 μm and have grown along the c-axis of the crystal structure of Zn_2GeO_4 as it was reported in a previous work [9]. Quantitative analysis of the EDS spectra shows that the structures are Zn_2GeO_4 with Mg concentration of 1.82 % in the case of doped samples, and in all cases, elements distribution is homogeneous along the samples.

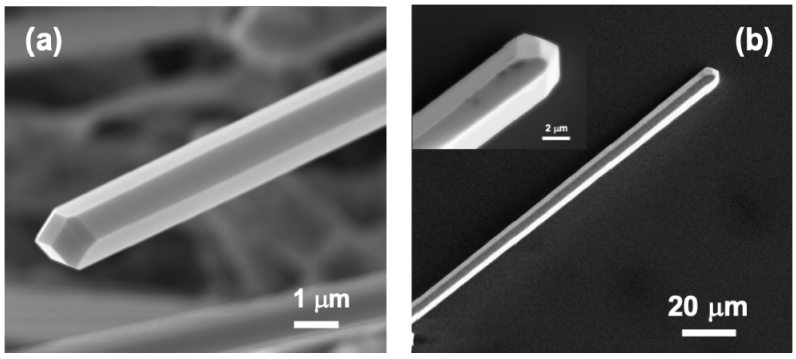

Figure 1.- SEM image of the undoped sample (a) and of a sample doped with Mg (b). The inset of the figure (b) shows a detail of the end of the microrod detailing its hexagonal structure.

Luminescence properties of undoped Zn_2GeO_4 microwires have been found to be highly dependent on the excitation conditions [3] [9]. PL spectra at RT and acquired under low excitation conditions in undoped samples show a broad band emission covering most of the visible range, from 1.6 eV to 3.3 eV with a maximum at 2.4 eV. This emission is a composed band of, at least three components peaked at 2.01 eV, 2.22 eV and 2.44 eV. Different works [16] propose that these emissions originate from oxygen defects and Ge centers that interact with Zn defects (interstitial or vacancies), but the mechanisms are not clear yet. When the excitation increases, an additional band at higher energy centered at approximately 3.23 eV is observed and becomes dominant in high excitation conditions [9]. On the other hand, CL emission of undoped samples only revealed this UV band. In this work, we present the luminescence by PL and CL of Mg doped Zn_2GeO_4 microwires in Figure 2. Figure 2(a) shows PL spectra of undoped and Mg doped samples for comparison. They show an intense UV band (at 3.3 eV) along with the visible broad band centered on 2.4 eV. Mg doped shows a markedly increase in the PL intensity and the dominant emission is the UV band under all excitation conditions. On the other hand, CL measurements also reveals a relevant increase of the output intensity for Mg doped samples. Figure 2(b) shows the CL spectrum of Mg doped Zn_2GeO_4 microwires recorded at 100 K. The deconvolution of the observed emission band reveals three components peaked at about 2.95 eV, 3.32 eV and 3.59 eV (inset in Figure 2(b)). The origins of these bands are not quite clear in the literature. EPR measurements have supported a model that would attribute this luminescence to donor-acceptor pair recombination with oxygen vacancies and zinc interstitials acting as donors and ionized germanium vacancies and zinc vacancies acting as acceptors [3]. Mg ions would enter into the Zn sublattice or as interstitial. In both cases, it would modify the landscape of native defects that are affecting the luminescence emission. Our PL and CL results show that an effective increase of luminescence intensity is clearly noticed, and in all cases, the dominant emission is the UV band, which appears to be a composed band.

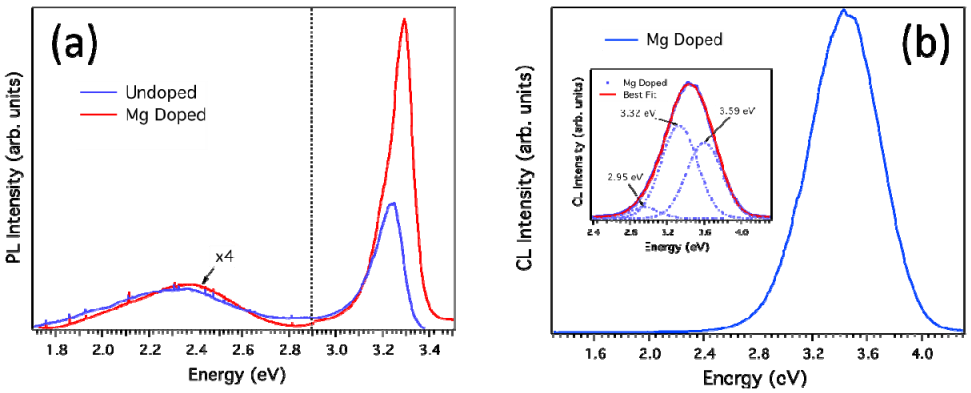

Figure 2.- (a) Room temperature PL spectra of undoped and Mg doped Zn_2GeO_4 microwires recorded under high excitation conditions. (b) CL spectrum of Mg doped Zn_2GeO_4 recorded at 100 K. Inset: Gaussian deconvolution of the luminescence bands.

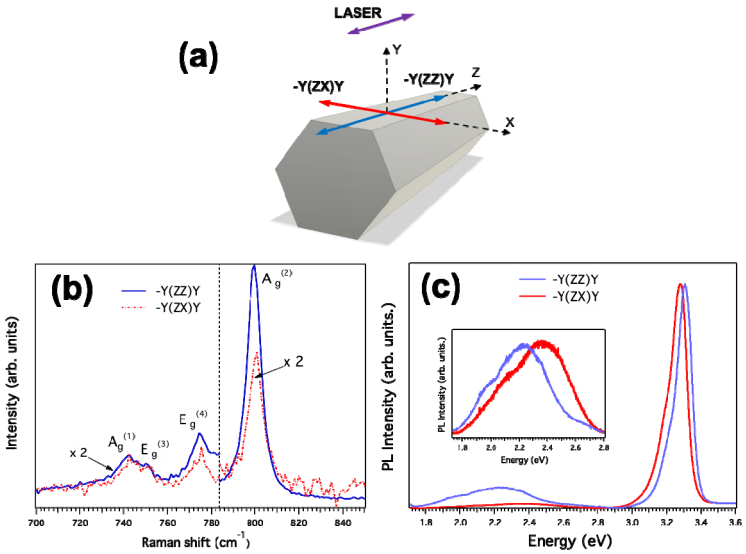

Figure 3.- (a) Sketch of the geometry for the polarized Raman and PL spectra of Mg-doped Zn_2GeO_4. The purple arrow indicates the polarization plane of the incident laser. Red and blue arrows indicate the polarizer orientation in the collection of the backscattered light. (b) Polarized Raman spectra and (c) polarized PL spectra, according to -Y(ZX)Y and -Y(ZZ)Y configurations. Inset in (c): Detail of the visible broad band.

In order to get an additional insight into the structural properties at local scale, we have performed polarized Raman spectroscopy measurements. The Raman spectrum from 700 to 840 cm^{-1} shows four characteristic bands assigned to the following vibration modes in the Zn_2GeO_4 lattice: Ge-O-Zn symmetric stretch, O-Ge-O bending defect oxygen mode, Ge-O-Zn asymmetric stretch and O-Ge-O stretching in the GeO_4 tetrahedra (see Table 1 for labeling and orientation). Raman spectra from undoped samples showed that relative intensity between modes changed as a function of the particular polarization orientation between the laser and the microwire. In particular, total and partial quenching of $E_g^{(4)}$ and $E_g^{(3)}$ modes, respectively, both perpendicular to *c*-axis, were attributed to the orientation of the wire along *c*-axis [17]. Figure 3(b) shows the polarized Raman spectra for Mg-doped samples recording the signal polarized parallel (-Y(ZZ)Y) or perpendicular (-Y(ZX)Y) to the longitudinal direction of the microrods. In this case, both E_g modes are excited in any of the configurations measured. This could be a hint about the location of Mg ions in the lattice. Concerning the $E_g^{(3)}$ mode, related to vibration modes in O-Ge-O, it could be possible that Mg ions sited at Zn lattice locations would do not affect this mode, and, hence its dependence on the polarization conditions is the same that in the undoped case. On the other hand, $E_g^{(4)}$ mode is not quenched in Mg-doped samples, even under polarization conditions that would imply that vibrations perpendicular to the *c*-axis would be affected. Therefore, we suggest that some Mg ions could be sited at the center of rings as an interstitial impurity, thus reducing the interstitial Zn concentration. This also would affect consequently the luminescence properties, since point defects are involved in the recombination centers.

Raman Mode	Mode Description	Raman Shift (cm^{-1})
$A_G^{(1)}$	Ge-O-Zn symmetric, ∥ c axis	745
$E_G^{(3)}$	O-Ge-O bending defect oxygen mode, ⊥ c axis	751
$E_G^{(4)}$	Ge-O-Zn asymmetric, ⊥ c axis	777
$A_G^{(2)}$	O-Ge-O stretching ∥ c axis	802

Table 1.- Description of Raman modes characteristic of Zn_2GeO_4 structure.

We have also correlated the polarized Raman measurement with polarized PL (p-PL) luminescence measurements in the optical confocal microscope. Figure 3(c) shows polarized PL spectra in Mg doped samples under polarization

configurations parallel and perpendicular to the microwire axis. We observe variations in the peak maxima position in both visible and UV emission bands when polarization conditions changes. The apparently shift of the visible band could be associated to changes in the ratio among their components, affecting most to the 2.44 eV component. This effect has also been observed in undoped samples and it has been linked to oxygen vacancies [17]. Concerning the UV emission, a clear shift to higher energies is detected by recording polarized light parallel to the microwire axis. Some authors have indicated that Zn_i donors are not essential in the emissions around 480-600 nm [12]. However, they could influence the UV emission. The fact that Mg doping could occupy zinc interstitial sites, as Raman measurements suggest, would agree with the fact that Mg_i related centers were mainly involved in the UV luminescence.

Finally, the waveguiding behavior of the Mg doped microrods has been assessed with the aid of a 325 nm laser. Figure 4 (a) shows an optical image of one microwire where the brightest with laser incident at one end and the bright spot at the other one. This is an indication of just light propagation along the wire. In addition, by laser excitation at the central part of the wire, we can get an image with the photoluminescence excited in the material. Figure 4(b) shows the micro-PL image in this case. The wire presents a permanent bluish luminescence resulting from the luminescence originated as the laser goes through the microwire. We suggest that this feature is due to the presence of Mg in interstitial position. A long-lasting photoluminescence (LLP) has been observed previously in Zn_2GeO_4 by Takahashi et al. [11]. They attributed this phenomenon to zinc in interstitial position that act as electron traps and conclude that Zn_i plays an important role for the LLP. Here, our results also suggest that Mg ions, in an interstitial position, are key factors for LLP in the UV region. The intensity profile along the wire shows some decay from the central part towards the ends of the wire, but the intensity again increases a little bit when reaching the ends of the wire (Figure 4(c)). Our confocal microscope set up allows to record PL spectra at a certain distance from the excitation point, in such a way that we can measure the spectrum of the guided light at the exit point, while keeping the generation point within the microwire. Figure 4(d) displays polarized PL spectra in –Y(ZX)Y configuration of emergent light from the excitation point and from point 2 (marked in Figure 4(b)). The results show that the UV is clearly composed of two components and both of them are collected at the excitation point (red line in Figure 4(d)). However, by collecting light at point 2, the 3.3 eV band is almost completely absorbed by the microwire. The UV emission is dominated by the 3.1 eV. This behavior has not been observed in undoped samples [9].

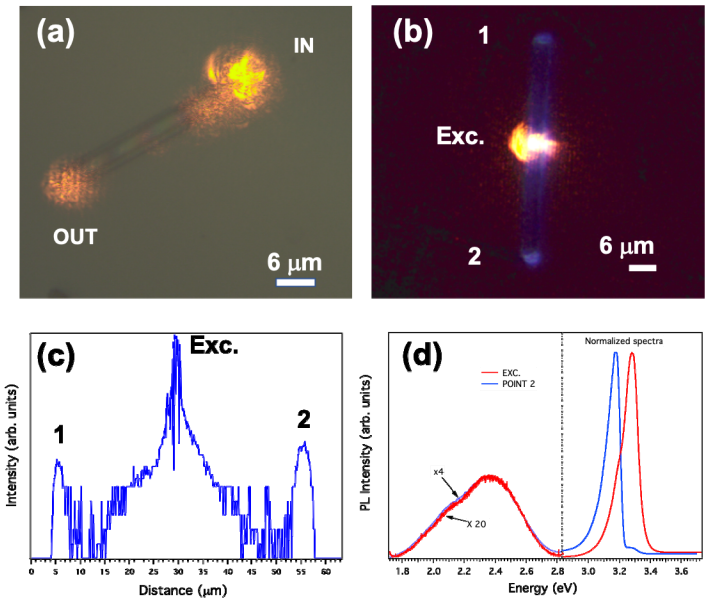

Figure 4.- (a) Optical images of an undoped wire showing the waveguiding behavior of the structure. (b) Mg doped microwire in dark field showing permanent luminescence. (c) Profile of the luminescence intensity along the rod shown in (b). (d) Normalized polarized PL spectra recorded at the generation point and at point 2 of the microwire shown in (b).

4. CONCLUSIONS

Undoped and Mg doped Zn_2GeO_4 microwires with lengths up to 100 microns and with hexagonal cross section have been grown by a vapor-solid method without the aid of any catalyst. Raman measurements and the analysis of the vibrational modes as a function of the polarization conditions suggest us that Mg could be incorporated as an interstitial ion in the structure. This could also influence the luminescence properties since point defects are involving in the DAP recombination centers of the material. We have found that Mg doped Zn_2GeO_4 presents significantly higher luminescence intensity than undoped microwires and show long-lasting photoluminescence. The luminescence shows a visible band in the green-yellow and an ultraviolet band, both of them of composed nature, which have been assessed by CL and PL measurements and found to be dependent on the excitation conditions. In particular, polarized PL measurements reveal that both emission bands show evident polarization effects. The luminescence results support the incorporation of Mg ions as well as interstitial, which would act as an electron trap, into the center of the rings of the structure. Further work will be needed to better clarify the mechanisms involved to explain all the luminescence bands observed in doped Zn_2GeO_4 microstructures.

ACKNOWLEDGEMENTS

This work has been supported by MIMECO projects MAT 2015-65274-R/FEDER and M-ERA.NET PCIN-2017-106

REFERENCES

[1] Hosono H. and Ueda K., *Springer Handbook of Electronic and Photonic Materials*. Cham: Springer International Publishing, 2017.

[2] Liu Z., Huang H., Liang B., Wang X., Wang Z., Chen D. and Shen G., "Zn_2GeO_4 and $In_2Ge_2O_7$ nanowire mats based ultraviolet photodetectors on rigid and flexible substrates," *Opt. Express*, vol. 20, no. 3, p. 2982, Jan. 2012.

[3] Liu Z., Jing X., and Wang L., "Luminescence of Native Defects in Zn_2GeO_4," *J. Electrochem. Soc.*, vol. 154, no. 6, pp. H500–H506, 2007.

[4] Liu L., Fan W., Zhao X., Sun H., Li P., and Sun L., "Surface dependence of CO_2 adsorption on Zn_2GeO_4," *Langmuir*, vol. 28, no. 28, pp. 10415–10424, 2012.

[5] Sato J., Kobayashi H., Ikarashi K., Saito N., Nishiyama H., and Inoue Y., "Photocatalytic Activity for Water Decomposition of RuO_2 -Dispersed Zn_2GeO_4 with d^{10} Configuration," *J. Phys. Chem. B*, vol. 108, pp. 4369–4375, 2004.

[6] Huang J., Wang X., Hou Y., Chen X., Wu L., and Fu X., "Degradation of benzene over a zinc germanate photocatalyst under ambient conditions," *Environ. Sci. Technol.*, vol. 42, no. 19, pp. 7387–7391, 2008.

[7] Bai Q., Li P., Wang Z., Xu S., Li T., Yang Z., Xu Z.., "Inducing tunable host luminescence in Zn_2GeO_4 tetrahedral materials via doping Cr^{3+}," *Spectrochim. Acta - Part A Mol. Biomol. Spectrosc.*, vol. 199, pp. 179–188, 2018.

[8] Feng J. K., Lai M. O., and Lu L., "Zn_2GeO_4 Nanorods synthesized by low-temperature hydrothermal growth for high-capacity anode of lithium battery," *Electrochem. commun.*, vol. 13, pp. 287–289, 2011.

[9] Hidalgo P., López A., Méndez B., and Piqueras J., "Synthesis and optical properties of Zn_2GeO_4 microrods," *Acta Mater.*, vol. 104, pp. 84–90, Feb. 2016.

[10] Joo Han K. and Kyung Ho Y., "Fabrication and Performance of ACTFEL Display Devices Using Manganese-Doped Zinc Germanate as a Green-Emitting Electroluminescent Layer," *J. Korean Phys. Soc.*, vol. 56, no. 6, p. 1861, 2010.

[11] Takahashi Y., Ando M., Iwasaki K., Masai H., and Fujiwara T., "Defect activation in willemite-type Zn_2GeO_4 by nanocrystallization," *Appl. Phys. Lett.*, vol. 97, no. 7, pp. 2–5, 2010.

[12] Wu S., Wang Z., Ouyang X., and Lin Z., "Core-shell Zn_2GeO_4 nanorods and their size-dependent photoluminescence properties.," *Nanoscale*, vol. 5, no. 24, pp. 12335–12341, 2013.

[13] Hidalgo P., Méndez B., and Piqueras J., "GeO_2 nanowires and nanoneedles grown by thermal deposition without

a catalyst," *Nanotechnology*, vol. 16, no. 11, pp. 2521–2524, 2005.
[14] Hidalgo P., Wilson Y., Ortega Y., and Piqueras J., "Synthesis, luminescence and micro-Raman study of $In_2Ge_2O_7$ nanobelts and nanowires," *Mater. Sci. Eng. B*, vol. 193, no. C, pp. 164–169, Mar. 2015.
[15] Zhao Y., Yang S., Zhu J., Ji G., and Peng F., "The study of oxygen ion motion in Zn_2GeO_4 by Raman spectroscopy," *Solid State Ionics*, vol. 274, no. 5, pp. 12–16, Jun. 2015.
[16] Li L., Su Y., Chen Y., Gao M., Chen Q., and Feng Y., "Synthesis and Photoluminescence Properties of Hierarchical Zinc Germanate Nanostructures," *Adv. Sci. Lett.*, vol. 3, no. 1, pp. 1–5, Mar. 2010.
[17] Dolado J., Hidalgo P. and Méndez B., "Correlative Study of Vibrational and Luminescence Properties of Zn_2GeO_4 Microrods," *Phys. status solidi*, vol. 215, no. 19, p. 1800270, Oct. 2018.